PHYSICAL REVIEW B, VOLUME 64, 235204

Atomic and electronic structures of a Boron impurity and its diffusion pathways in crystalline Si

Ji-Wook Jeong* and Atsushi Oshiyama

Institute of Physics, University of Tsukuba, 1-1-1 Tennodai, Tsukuba 305-8571, Japan

(Received 4 June 2001; published 15 November 2001)

We present extensive first-principles total-energy calculations for boron-silicon interstitial complexes with various configurations and charge states within the density functional theory. We find several stable and metastable configurations. We also find that the stability of each configuration is sensitive to its charge state: The most stable configuration is a pair of a substitutional B and an interstitial Si for positively charged state, whereas an interstitialcy configuration is the most stable for negatively charged state. The pair and the interstitialcy configurations have almost same formation energies in their neutral charge states. Examination of electron states induced by the B-Si complexes indicates that the neutral interstitialcy configuration is an active center for electron spin resonance measurements. It is also found that the B-Si complex is a negative-U system in which neutral charge states are only metastable with the Fermi energy at any position in the energy gap, corroborating the earlier experimental finding by Watkins and collaborators. Further, we present diffusion pathways and corresponding activation energies for the B-Si complex. It is found that the pathways and the activation energies are again sensitive to the charge state, opening a possibility of recombination enhanced diffusion. The calculated results are compared quantitatively with experiments and previous calculations available.

DOI: 10.1103/PhysRevB.64.235204 PACS number(s): 66.30.Jt, 71.55.−i, 61.72.−y, 85.40.Ry

I. INTRODUCTION

Atomic diffusion is an important phenomenon in condensed matters. Dopant diffusion in Si crystal, for instance, plays a central role in fabrications of electronic devices: Modeling of diffusion profiles of the dopant impurities is imperative for design of the devices. The modeling, on the other hand, crucially depends on underlying diffusion mechanisms. Microscopic identification of the diffusion mechanism is thus important and challenging in semiconductor science and technology. There have been a lot of efforts to clarify macroscopic and microscopic aspects of the diffusion phenomenon.[1–3] It is now recognized that the atomic diffusion in Si takes place with the aid of intrinsic point defects, i.e., the self-interstitials (Si_i) or the vacancies (V). In the interstitial or the interstitialcy mechanisms the diffusing species migrates in the interstitial region with or without the self-interstitial, whereas in the vacancy mechanism it migrates in the form of a pair with the vacancy. Another mechanism in which intrinsic defects are not involved and host atoms assist in the diffusion concertedly is also proposed.[4,5] Yet a variety of experiments[1–3] that shows correlation between the concentrations of the intrinsic defects and the diffusivity clearly indicates important roles of point defects.

Theoretical efforts to identify the mechanism which is responsible for the diffusion of each atomic species have been done for years. An earlier calculation[6] based on the density functional theory and subsequent theoretical efforts[7] have revealed that both the interstitial and the vacancy mechanisms are important for the self-diffusion in Si. Systematic calculations for the dopant diffusion have clarified chemical trends in relative importance of the respective mechanisms for each dopant impurity.[7–9] Calculations of diffusion constants[10] and several experimental efforts[11–14] have certainly enriched our knowledge about the mechanisms.

As for boron that is an acceptor most commonly used in Si, the mechanism responsible for the diffusion is relatively clear: B diffusivity is enhanced by the self-interstitials and retarded by the vacancies.[15,16] Boron is then considered to diffuse via the kick-out mechanism in which the self-interstitial kicks out B at a substitutional site (B_s) and then the B migrates in the interstitial region (B_i) until it is kicked in another substitutional site. Calculations of migration barriers[7,17–19] seem to corroborate this picture of kick-out and kick-in processes. Yet another possibility that B diffuses as a pair of B and the self-interstitial has been proposed recently[20,21] based on the density functional calculations using the VASP code disseminated:[22] Sadigh *et al.*[20] and Windl *et al.*[21] have found that B_s forms a pair with the self-interstitial at the tetrahedral site (B_s-Si_i^T), and diffuses via some saddle point geometries where the pair is not dissociated. The stability of a pair of B_s and Si_i has been also reported in an earlier calculation[23] and in a recent LDA calculation.[24]

On the other hand, a foreign atom in a semiconductor generally induces deep levels in the forbidden region of energy bands (energy gap) of the host material due to the loss of translational symmetry in an otherwise perfect crystal. An important characteristic of the deep level in semiconductors is that the deep level traps carriers. As a result of this, the foreign atom (or generally the deep center) takes different charge states depending on the Fermi-level position in the energy gap. Energy change upon accommodation of an additional electron in the deep level is usually positive due to Coulomb interaction U among the electrons in the deep level. Yet the energy change could be negative when lattice relaxation which depends on the deep-level charge state is large enough to compensate the Coulombic repulsion.[25] The vacancy in Si crystal is predicted to be such a negative-U system based on the density-functional Green's-function calculation.[26] Experimentally, the boron impurity in Si crystal is shown to be the negative-U system,[27–29] based on the

 ©2001 The American Physical Society

electron-paramagnetic-resonance (EPR) measurement,[27] the deep-level-transient-spectroscopic (DLTS) measurement,[27] and the photogenerated DLTS measurement.[28]

In this paper we present our total-energy electronic-structure calculations performed for stable structures, diffusion pathways and the activation energies for the B impurity in Si. Regarding the diffusion pathways, our results complement the microscopic pictures obtained by Sadigh *et al.*[20] and by Windl *et al.*:[21] We confirm that the pair B_s-Si_i^T is stable for positively charged and neutral states. Yet we find that there are another pathways along which the activation energies are comparable or less compared with the values obtained before. Further it is found that recombination of carriers at deep levels enhances the B diffusivity. As for the electronic structure, we find that B in Si is a negative-U system, consistent with the experiments by Watkins and his collaborators.[27,28] We find that for the negatively charged state a new interstitialcy configuration is the most stable. This interstitialcy configuration is metastable for the neutral charge state, only 70 meV higher in energy than the most stable neutral configuration. We identify this interstitialcy configuration is the EPR center experimentally observed. Detailed analyses of the level structures and wavefunctions for several relevant metastable geometries provide a theoretical framework to discuss electronic structures of B in Si.

In Sec. II, the calculational method is described. Results obtained for atomic and electronic structures and for the diffusion mechanisms are presented in Sec. III. Section IV concludes the paper.

II. THEORETICAL METHOD

All calculations have been performed in the density functional theory.[30] Nuclei and core electrons are simulated by norm-conserving pseudopotentials.[31] We adopt prescriptions by Troullier and Martins[32] to generate actual pseudopotentials. Nonlocal parts of the pseudopotentials are transformed in separable forms of Kleinman and Bylander.[33] Exchange and correlation energies among valence electrons are treated in the local density approximation (LDA) and in the generalized gradient approximation (GGA).[34] In the LDA, we use the functional form by Perdew and Zunger[35] fitted to the results for the homogeneous electron gas obtained by quantum Monte Carlo method.[36] The GGA is considered to be a better approximation than the LDA. Yet we present values not only from the GGA but also from the LDA in this paper since the comparison would be beneficial to assess each approximation. To expand the wave functions, the plane-wave basis set with the cutoff energy of 28 Ry is used.[37] Boron-related defects in an otherwise perfect Si crystal is simulated by a supercell model in which cubic cells containing 64 lattice sites are arranged periodically. We use theoretical lattice constants, 5.38 Å in the LDA and 5.50 Å in the GGA, for the cubic cell. For the k-point sampling in the Brillouin zone, a uniform grid of k points equivalent to $2\times2\times2$ Monkhorst and Pack grid in the diamond cubic supercell is used. Both the electronic and ionic degrees of freedom are optimized in the total-energy minimization by the highly efficient conjugate gradient method.[38–40] For the structure optimization, all atoms are fully relaxed without restricting the symmetry.

The formation energy E_f^Q of a B-related defect D with its charge state $Q(=\pm1,\dots)$ is expressed as

$$E_f^Q=(E_D^Q-E_X^0)+Q(\varepsilon_F+\varepsilon_v)-\sum_s\,(n_s^{(D)}-n_s^{(X)})\mu_s, \quad (1)$$

where E_D^Q is the calculated total energy of the supercell containing the defect D, E_X^0 is the total energy of the corresponding perfect "crystal" supercell, and μ_s is the chemical potential of the atomic species s. $n_s^{(D)}$ and $n_s^{(X)}$ are the number of the atoms in the supercell with and without the defect, respectively. When we consider the formation energies of the B-related defect in Si, we need the chemical potential of B and Si, μ_B and μ_{Si}. Yet we restrict ourselves in this paper to the defects containing a single B atom so that μ_B is not required to obtain relative formation energies of the defects. As for μ_{Si}, we take the total energy per atom of bulk Si crystal.

The formation-energy difference between different charge states generally depends on the electron chemical potential (i.e., the Fermi level) ε_F. In Eq. (1), ε_F is measured from the valence-band top ε_v, whereas ε_v is relative to the vacuum. From Eq. (1) we obtain

$$E_f^{\pm1}-E_f^0=(E_D^{\pm1}-E_D^0)\pm(\varepsilon_F+\varepsilon_v). \quad (2)$$

In the supercell model with the plane-wave basis set, the total-energy difference between different charge states, as in the right hand side of Eq. (2), is not easy to compute accurately. We thus utilize the fact that the minus ε_v is the first ionization energy of the semiconductor and is expressed as[41]

$$\varepsilon_v=E_{crys}^0-E_{crys}^{+1}, \quad (3)$$

where E_{crys}^0 is the total energy of the perfect crystal and E_{crys}^+ is the corresponding total energy with the highest occupied state (i.e., the valence-band-top state) being empty. The right hand side of Eq. (3) is evaluated by the supercell model as

$$E_{crys}^0-E_{crys}^{+1}=E_X^0-E_X^{+1} \quad (4)$$

in this paper. Then the formation-energy difference between the positive and neutral charge states becomes

$$E_f^{+1}-E_f^0=(E_D^{+1}-E_X^{+1})-(E_D^0-E_X^0)+\varepsilon_F, \quad (5)$$

which can be computed with high accuracy.

As for the negative charge state, we encounter the band-gap problem in the LDA and the GGA. A simple manipulation similar to the above leads to

$$E_f^{-1}-E_f^0=(E_D^{-1}-E_X^{-1})-(E_D^0-E_X^0)-\varepsilon_F+\varepsilon_{N+1}^{N+1}-\varepsilon_N^N, \quad (6)$$

where ε_M^M is the Mth Kohn-Sham eigenvalue in the M-electron system. The ε_N^N is thus equal to ε_v and $\varepsilon_{N+1}^{N+1}-\varepsilon_N^N$ is regarded as the band gap of the semiconductor. Since both the LDA and the GGA underestimates the band gap substantially, $\varepsilon_{N+1}^{N+1}-\varepsilon_N^N$ is unable to be evaluated accurately in the present theoretical framework. We thus adopt in this

paper a practical strategy in which $\varepsilon_{N+1}^{N+1}-\varepsilon_N^N$ in Eq. (6) is replaced by the experimental band gap, 1.2 eV. Equations (5) and (6), along with Eq. (1) for the neutral charge state, are utilized to evaluate the formation energies in this paper.

The treatment above to circumvent the band-gap problem in the DFT should be regarded as inconclusive. When we use the DFT band gap instead of the experimental band gap, the formation energy for the negative charge state shift downward by a half eV relative to those for the neutral and positive charge states. Alternatively, we may use Slater's transition-state idea[42,43] in which the total-energy difference between the different charge states is evaluated by the Kohn-Sham eigen values with partial occupation. This treatment is also unable to be free from the band gap problem. We believe that the present treatment with the experimental band gap is the best at present to assess the formation energy for the negative charge state.

In the supercell model for charged defects, we usually put homogeneous countercharge to keep neutrality of the supercell. This treatment causes an error in computing total energies for the charged defect. We have thus included a correction for the electrostatic energy which results from the charged defect and the countercharge in the supercell model. Using the dielectric constant ϵ of Si, and the Madelung constant α for the diamond structure with the lattice constant of the cubic supercell a_0, the correction could be written as

$$+\frac{e^2Q^2\alpha}{a_0\epsilon}.$$

The typical value for the correction is 0.16–0.17 eV for the singly charged defect in the present work.

Obtaining the diffusion pathways of the boron-related defect is a task to find valleys of the multidimensional total energy surface. To accomplish the task, we adopt the constraint minimization method.[44] We first perform extensive searches of (meta)stable geometries of the boron-related defect in the L-dimensional space where L is the ionic degrees of freedom to be considered. Then we take two of the (meta)stable geometries and explore a plausible diffusion pathway between the two geometries as follows: We first define a $(L-1)$-dimensional plane which is perpendicular to the L-dimensional vector connecting the two (meta)stable geometries; we perform the geometry minimization within the $(L-1)$-dimensional plane to find the minimum point on the plane; we repeat the constraint minimization on several planes perpendicular to the vector; we then finally obtain a plausible pathway between the two (meta)stable geometries and the corresponding activation energy. We have carried out the procedure for all the relevant pairs of the (meta)stable geometries so that we have reached a complete landscape of the diffusion pathways.[45]

III. RESULTS AND DISCUSSION

A. Atomic structures and formation energies of boron-related defects

We have found that three different charge states (neutral, +1 and −1 states) are possible for a boron in Si with a variety of bonding configurations. Among them, the most stable form for the B is a substitutional site (B_s). Our calculations show that a negatively charged substitutional B (B_s^-) is the lowest in energy for any value of the electron chemical potential (ε_F) in the gap. This corresponds to the fact that a boron atom is a good acceptor in Si, being located at a substitutional site. In this paper, we present formation energies of B-related defects as a function of ε_F with respect to the energy of B_s^-.

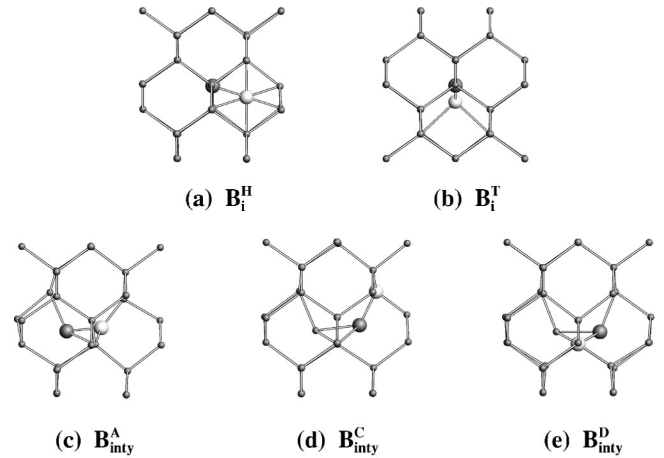

FIG. 1. Stable and metastable atomic configurations of a boron impurity. (a) Boron at hexagonal interstitial site (B_i^H), (b) boron at tetrahedral interstitial site (B_i^T), (c) an interstitialcy configuration A (B_{inty}^A) in which the B-Si interstitialcy bond is located on the $(1\bar{1}0)$ plane with the [110] direction, (d) an interstitialcy configuration C (B_{inty}^C) in which the B-Si interstitialcy bond is located on the $(1\bar{1}0)$ plane with the [112] direction, and (e) an interstitialcy configuration D (B_{inty}^D) in which the B-Si interstitialcy bond is located on the $(1\bar{1}0)$ plane with the $[\bar{1}51]$ direction. Large brighter balls depict B atoms, whereas large darker balls and small balls do Si atoms.

We have performed extensive searches for (meta)stable geometries of a B interstitial configuration (B_i) and of a pair of a B and a Si interstitial (B_s-Si_i), as well as an interstitialcy configuration (B_{inty}) in which both B and Si are dislodged from lattice sites.

Figures 1(a) and 1(b) show two of B_i configurations: B at an interstitial site with hexagonal symmetry (B_i^H) and B at a site with tetrahedral symmetry (B_i^T). An important interstitialcy configuration is labeled B_{inty}^A [Fig. 1(c)] in which the interstitialcy B-Si bond is located on the $(1\bar{1}0)$ plane with the [110] bond direction. We have also found two additional metastable interstitialcy configurations labeled B_{inty}^C [Fig. 1(d)] and B_{inty}^D [Fig. 1(e)]. All these configurations are found to be (meta)stable in the present LDA and the GGA calculations. Yet the relative stability depends on their charge states, as will be explained below. We have also found that pairs of a substitutional B and a Si self-interstitial are also stable. Figure 2 shows two (meta)stable pairs: In Fig. 2(a), a Si self-interstitial is located near a tetrahedral interstitial site next to the boron (B_s-Si_i^T), whereas in Fig. 2(b) it is located near another tetrahedral site next to a Si atom bonded to the boron (B_s-$Si_i^{T'}$).

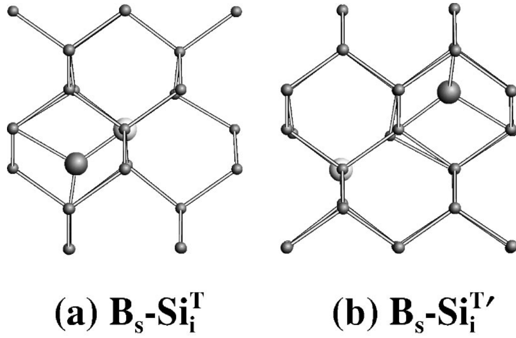

FIG. 2. Stable and metastable pairs of a substitutional boron and a Si self-interstitial. (a) Si self-interstitial is located near a tetrahedral interstitial site next to the boron (B_s-Si_i^T). (b) Si self-interstitial is located near a tetrahedral interstitial site next to another Si bonded to boron (B_s-$Si_i^{T'}$). Large brighter balls depict B atoms, whereas large darker balls and small balls do Si atoms.

In the neutral charge state, the most stable configuration that we have found is the pair B_s-Si_i^T. Its formation energy with respect to the negatively charged substitutional boron B_s^- is 2.5 (2.1) eV when ε_F is at the top of valence bands ε_v. Here and hereafter, energy values presented are obtained from the GGA, whereas values in the parentheses are from the LDA. The calculated formation energy for the pair B_s-Si_i^T is compared to the values obtained in the past: 2.8 eV (2.5 eV) in the GGA (LDA) (Ref. 21) and 2.48 eV in the LDA.[24] We provisionally ascribe the difference of a few tenths of eV in the formation energy to the different treatment for the negative charge state described in the previous section. We have also calculated a binding energy of B_s-Si_i^T with respect to an isolated B_s^- and Si_i^{T+}. The obtained value is 0.7 (0.6) eV which is comparable to the values in the past: 0.8 (0.5) eV.[21] It is of interest that the obtained value is close to the sheer Coulombic attraction between $+e$ and $-e$ point charges ($\sim$0.6 eV). Zhu *et al.*[17] have proposed another metastable pair configuration B_s-$Si_i^{T'}$ where the Si interstitial is located at another tetrahedral interstitial site in the opposite side of a B-Si bond [Fig. 2(b)]. The present calculation shows that the formation energy of B_s-$Si_i^{T'}$ is higher than that of B_s-Si_i^T by 0.17 (0.13) eV. This value of 0.13 eV in the LDA reasonably agrees with the previous value 0.1 eV by Zhu *et al.* The B interstitial and interstitialcy configurations (B_i^H, B_i^T, B_{inty}^A, B_{inty}^C, and B_{inty}^D) are also metastable. The calculated formation energies are shown in Table I. The values are higher than that of B_s-Si_i^T by typically a half eV. Yet it is noteworthy that the formation energy of B_{inty}^A is close to that of B_s-Si_i^T, higher only by 70 meV in the GGA. This implies that a substantial portion of boron takes the form of B_{inty}^A when it is neutral.

For positively charged states, the pair B_s-Si_i^{T+} is again most stable. Its binding energy with respect to an isolated B_s^- and Si_i^{T++} is 0.9 (0.8) eV, increasing compared with the neutral state. The present values are comparable with those obtained in the previous calculations 1.0 eV (0.8 eV) in the GGA (LDA) (Ref. 21) and 1.03 eV (0.90 eV) in the GGA (LDA).[20] The formation energy of B_s-$Si_i^{T'+}$ is found to be 0.23 (0.16) eV higher than that of B_s-Si_i^{T+}. Some of the interstitial configurations are also metastable in the positively charged state (Table I). The formation energies are about 0.7–1.0 eV higher than that of the most stable geometry B_s-Si_i^{T+}. The interstitialcy configuration B_{inty}^{A+} becomes unstable, however: It spontaneously changes its form to B_s-Si_i^{T+}.

For negatively charged states, the pair B_s-Si_i^T becomes metastable. The most stable geometry is the interstitialcy configuration B_{inty}^{A-}. It is lower than B_s-Si_i^{T-} in formation energy by 0.39 (0.17) eV. The binding energy of B_{inty}^{A-} with respect to an isolated B_s^- plus neutral Si at the interstitialcy configuration A is 0.4 (0.2) eV. The most stable geometry B_{inty}^{A-} that we have found may be similar to the geometries discussed previously (Fig. 1 in Ref. 24 or Fig. 5 in Ref. 23), although the quantified examination of the similarity is not feasible now. On the other hand, B_{inty}^{A-} is different from the geometry B_i^{X-} which has been identified previously as the most stable configuration for the negatively charged state (Fig. 1 in Ref. 21): The calculated formation energy for B_i^{X-} is higher than that for B_{inty}^{A-} by 0.38 (0.17) eV in the present calculation. Further, the B at the hexagonal site (B_i^H) which was identified as the most stable form for the negatively charged state by Zhu[18,19] is found to be higher in formation energy than B_{inty}^{A-} by 0.26 (0.29) eV. The extensive search for the stable configurations performed here allows us to reach the most stable configuration B_{inty}^{A-}.

TABLE I. Formation energies of B-related defects with different charge states. Energies are in unit of eV and relative to the energy of the most stable configuration for each charge state. Calculated values from the GGA and from the LDA (in parentheses) are shown. The previous values in literature are also shown for comparison. The configurations B_{inty}^S, $B_{inty}^{S'}$ are the saddle point configurations, and the rest of the configurations are (meta)stable. B_{inty}^{A+} and B_{inty}^{C+} are found to be unstable, therefore denoted by the short dashed lines.

	+1	0	−1
B_s-Si_i^T	0.00 (0.00)	0.00 (0.00)	0.39 (0.17)
B_s-$Si_i^{T'}$	0.23 (0.16)	0.17 (0.13)	0.49 (0.17)
		(0.1) [a]	
B_{inty}^A		0.07 (0.20)	0.00 (0.00)
B_{inty}^C		0.54 (0.53)	0.20 (0.11)
B_{inty}^D	1.37 (1.28)	0.56 (0.55)	0.18 (0.05)
B_i^T	0.72 (0.97)	0.63 (0.89)	1.13 (1.28)
	(0.87) [b], (0.98) [c]	(0.7) [a], (0.82) [b]	
B_i^H	0.95 (1.01)	0.35 (0.51)	0.26 (0.29)
	(0.93) [b], (1.14) [c]	0.4 [a], (0.41) [b], (0.58) [c]	
$B_{inty}^{S'}$	0.94 (1.01)	0.52 (0.75)	0.32 (0.41)
B_{inty}^S	0.46 (0.80)	0.32 (0.62)	0.62 (0.72)

[a]Reference 17.
[b]Reference 20.
[c]Reference 24.

Table I shows calculated formation energies of B-related defects with +1, 0, and −1 charge states in the GGA and in the LDA. The values obtained in the past are also shown. The formation energies of the (meta)stable geometries obtained in the present calculations agree with the previous DFT values within about 0.1 eV. This discrepancy of 0.1 eV is presumably due to calculational parameters such as the cutoff energy of the basis set or the *k*-point sampling, and is typical in the DFT calculations. It is also noticed that the LDA and the GGA provide similar values for metastable geometries. For the formation energies for saddle-point geometries ($B^{S}_{\rm inty}$ and $B^{S'}_{\rm inty}$), however, the differences between the GGA and the LDA values are sizable. Therefore in determination of diffusion barriers and corresponding activation energies, the LDA alone may be insufficient (see also Fig. 5).

B. Electronic structures of boron-related defects

In this subsection, we present electronic structures obtained from the total-energy calculations performed for the Boron-related defects, and discuss their negative-U characters originally found in the pioneer experiments by Watkins and his collaborators.[27–29]

Figure 3 is an excerpt from the present total energy calculations for a variety of B-related defects described above for positively charged, neutral and negatively charged states as a function of Fermi level (ε_F) in the energy gap. From Fig. 3, we obtain the occupancy level or the thermodynamic level $\varepsilon(Q/Q')$, which is defined in the following statement: When the Fermi level ε_F is lower (higher) than $\varepsilon(Q/Q')$, the stable charge state is $Q(Q')$. Our GGA calculations [Fig. 3(b)] show that $\varepsilon(+/-)$ is located at $\varepsilon_v+0.9$ eV. Neutral charge states are found to be only metastable in the GGA at any position of ε_F in the gap. As stated above, the most stable geometry for +1 charge state is the pair B_s-Si^T_i, whereas it is $B^A_{\rm inty}$ for −1 charge state. The results from the LDA calculations [Fig. 3(a)] are qualitatively same as but quantitatively different from the GGA results. In the LDA, we find a narrow range of 0.12 eV in the gap where the neutral B_s-Si^T_i is the most stable. The previous LDA calculation[24] for the B_s-Si^T_i shows that the neutral state is metastable. The present LDA result disagrees at this point. Yet, when we use the DFT band gap instead of the experimental band gap in Eq. (6), the present LDA calculation also indicates that the neutral state is metastable. In any case, since the GGA is better in principle than the LDA, it is safely concluded from the present DFT calculations that the B-related defect in Si is a negative-U system in which the neutral state is always metastable at any position of ε_F in the energy gap.

The EPR experiment[29] on Boron in Si has observed a signal named Si-G28. From the loss of the Si-G28 upon annealing, a donor level $\varepsilon(+/0)$ is evaluated to be located at $\varepsilon_c-0.15$ eV where ε_c is the conduction-band bottom. The position of the donor level has been later corrected to be $\varepsilon_c-0.13$ eV, and further the donor level is observed also by the photogenerated DLTS experiment.[28] Electron emission from the negative charge state has also been observed by the DLTS experiments.[27] From the analysis of the emission rate, the acceptor level $\varepsilon(0/-)$ is evaluated to be $\varepsilon_c-0.45$ eV,[27] and is later corrected to be $\varepsilon_c-0.37$ eV on account of the Poole-Frenkel effect.[28] From this series of experiments, it is concluded that the B-related defect in Si is a negative-U system. The Hubbard U experimentally determined is thus $U\equiv\varepsilon(0/-)-\varepsilon(+/0)=-0.24$ eV.

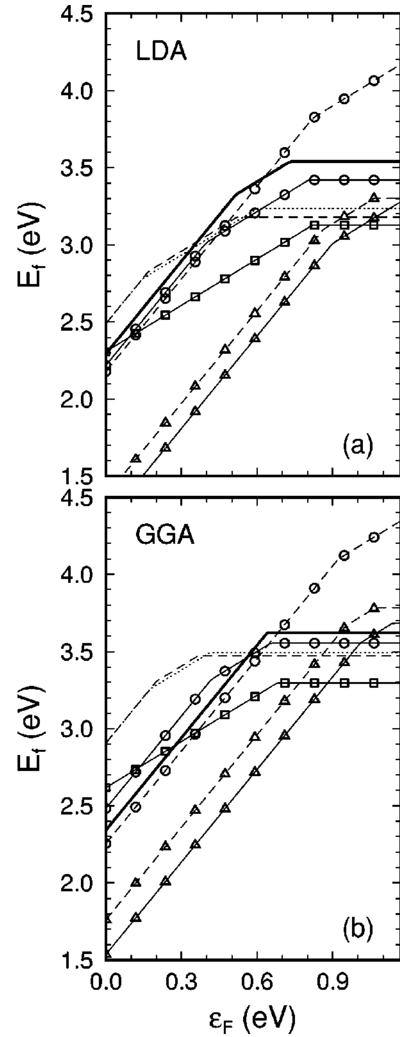

FIG. 3. Calculated formation energies of a variety of B-related defects for positively charged (positively slanted lines with the slope of $2\epsilon_F$), neutral (positively slanted lines with the slope of ϵ_F), and negatively charged (horizontal lines) states as a function of Fermi level (ε_F). (a) The LDA results and (b) the GGA results. All the formation energies are measured from that of B_s^-. The formation energies of B_s-Si^T_i, B_s-$Si^{T'}_i$, $B^A_{\rm inty}$, $B^C_{\rm inty}$, $B^D_{\rm inty}$, B^H_i, and B^T_i are shown by the solid line with triangles, the dashed line with triangles, the solid line with squares, the dotted line, the dashed line, the solid line with circles, and the dashed line with circles, respectively. The formation energy of the saddle point geometry is drawn by the thick solid line.

From the GGA calculation in Fig. 3, we obtain $\varepsilon(0/-)=\varepsilon_v+0.7$ eV and $\varepsilon(+/0)=\varepsilon_v+1.1$ eV. Here we identify the neutral center observed by the EPR and the photogenerated DLTS measurements as our neutral $B^A_{\rm inty}$. This identification will be explained with the analysis of the wave func-

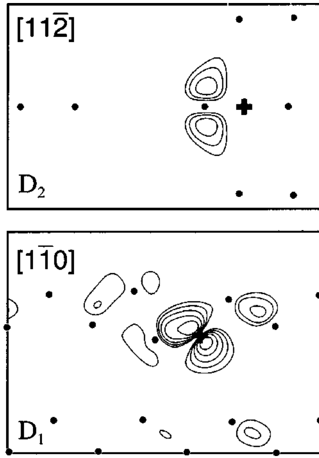

FIG. 4. Calculated charge densities of the deep Kohn-Sham levels D_1 and D_2 induced by the B^A_{inty} in Si. D_1 is lower than D_2 in energy. Silicon atoms are drawn by black balls and boron atoms by crosses. The charge density value for the highest contour line is 0.045 (Å^{-3}) and the subsequent lines increase by a factor of 1.86 (decrease by a factor of 0.54).

tions of the deep levels later. Hence the theoretical estimate of the Hubbard U is $-$ 0.4 eV in reasonable agreement with the experimental value. Also the theoretical positions of $\varepsilon(0/-)$ and $\varepsilon(+/0)$ are in accord with the experimental values. The agreement is not conclusive, however. When we take the DFT band gap in Eq. (6) in our GGA calculations, $\varepsilon(0/-)$ shifts downward to be about ε_v plus a few tenths of eV. A new calculational scheme beyond the DFT is certainly required to determine the positions of the occupancy levels accurately.

The Kohn-Sham (KS) energy levels and the corresponding KS orbitals are not exactly related to the occupancy levels. Further, it may be ambiguous to identify each KS energy level as a deep level, resonant level, or continuum level, when we examine the location of the energy level only, since all the levels have dispersion in principle in the supercell model. Examination of corresponding KS orbitals, however, allows us to clarify the chemical nature of each KS level, and then characteristics of the corresponding occupancy level.

For B_s-Si_i^T, we observe no deep KS levels in the energy gap. This is interpreted as follows. It is known that the Si self-interstitial at a tetrahedral site induces no deep levels: a state with symmetry a_1 is located below the valence bandtop and triply degenerate states with symmetry t_2 are above the conduction-band bottom.[6] When a nearest neighbor Si of the Si self-interstitial is replaced with B, we reach B_s-Si_i^T configuration. This replacement does not induce a new deep level but splits the triply degenerate level to a doubly degenerate level and a single level since the symmetry changes from T_d to C_{3v}. The resulting doubly degenerate level becomes close to the conduction-band bottom. Yet the splitting is not so large that the doubly degenerate level is still resonant or is shallow below the conduction bands. Further, the KS orbitals of these levels have the amplitudes not only on the boron site but also on the Si at the tetrahedral site and on its nearest neighbor Si sites. The EPR signal Si-G28 lacks the symmetry of C_{3v} and the wave function is mainly located at the boron site.[29] It is therefore unlikely that the B_s-Si_i^{T0} is the neutral center observed by the EPR experiment.

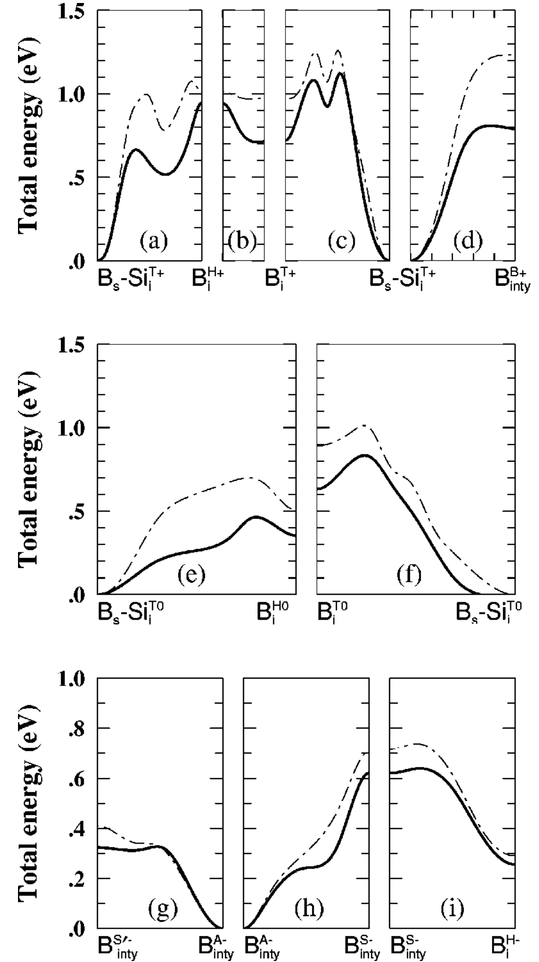

FIG. 5. Total energy profiles along diffusion pathways for B. Thick solid lines are from the GGA calculations and thin dot-dashed lines are from the LDA calculations. The profiles are (a) between B_s-Si_i^{T+} and B_i^{H+}, (b) between B_i^{H+} and B_i^{T+}, (c) between B_s-Si_i^{T+} and B_i^{T+}, (d) between B_s-Si_i^{T+} and B_i^{B+}, (e) between B_s-Si_i^{T0} and B_i^{H0}, (f) between B_s-Si_i^{T0} and B_i^{T0}, (g) between B^{A-}_{inty} and $B^{S'-}_{inty}$, (h) between B^{A-}_{inty} and B^{S-}_{inty}, and (i) between B^{S-}_{inty} and B_i^{H-}. Energies are measured from that of the most stable geometry for each charge state.

On the contrary, B^A_{inty} induces two deep KS levels. Figure 4 shows calculated KS orbitals for the two deep levels. It is clear that the orbitals are localized near the bond-distorted region and mainly on the boron site. In the neutral charge state, the lower deep level D_1 is occupied by an electron. Therefore the neutral B^A_{inty} is EPR active. The symmetry of neutral B^A_{inty} is C_{1h} which is in accord with the EPR experiment. From these results, we argue that the observed EPR center is the neutral B^A_{inty} which is metastable, higher in energy by 70 meV than the neutral B_s-Si_i^T.

As shown in the next subsection (Fig. 5), the migration or the reaction energy barriers from B^A_{inty} to B_s-Si_i^T via another interstitialcy configuration is about a half eV. This may cor-

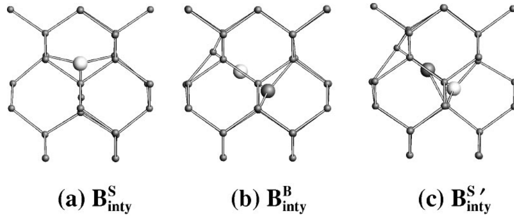

FIG. 6. Atomic configurations which appear during B diffusion. (a) B_{inty}^{S}, (b) B_{inty}^{B}, and (c) $B_{inty}^{S'}$. Large brighter balls depict B atoms, whereas large darker balls and small balls do Si atoms.

respond to the observed reorientation or the diffusing-away barriers of the EPR center, which are both estimated to be 0.6 eV.[29]

C. Mechanism of boron diffusion

We are now in a position to discuss mechanisms of boron diffusion. We have identified several (meta)stable configurations for the B-related defect. Then we next search diffusion pathways for a B atom.

Let us start with the diffusion of positively charged B. The most stable geometry is B_s-Si_i^{T+} so that the geometry is the starting point for the diffusion. We have first examined a process in which the B in the B_s-Si_i^{T+} is kicked out to a nearby interstitial site. Figures 5(a), 5(b), and 5(c) show the calculated results. We have found one and two peaks, respectively, in energy profiles along a path from B_s-Si_i^{T+} to B_i^{H+} and B_i^{T+}. We have found a local minimum along a path from B_s-Si_i^{T+} to B_i^{H+}. This minimum configuration is labeled as B_{inty}^{S} [Fig. 6(a)]. This B_{inty}^{S} is similar to the configuration obtained by the recent GGA calculations[21] (labeled as B_i^S in Ref. 21).

The activation energy from B_s-Si_i^{T+} to B_i^{H+} is 0.95 (1.08) eV in the present calculations. On the other hand, the activation energy from B_s-Si_i^{T+} to B_i^{T+} is found to be 1.12 (1.26) eV. It is thus likely that B migrate mainly along a path from B_s-Si_i^{T+} to B_i^{H+}. The total energy for B_i^{T+} is lower than that for B_i^{H+} by 0.23 (0.04) eV and there is no additional energy barrier between the two configurations [Fig. 5(b)]. Therefore, once B is kicked out from B_s-Si_i^{T+} to B_i^{H+}, B athermally migrates to the nearby tetrahedral interstitial site, and only 0.23 (0.04) eV is required to move along a channel through the hexagonal and tetrahedral interstitial sites (kick-out mechanism). Yet a kick-in barrier is 0.15 (0.22) eV [Fig. 5(a)] so that a long-distance migration via the kick-out mechanism is unlikely. On the other hand, the pair diffusion mechanism in which B_s-Si_i^{T+} becomes B_i^{H+} and then becomes another B_s-Si_i^{T+} provides the activation energy of 0.95 (1.08) eV.

Another pathway may be a bond-center path in which the saddle point is an interstitial B located at the bond-centered site [B_{inty}^{B+} depicted in Fig. 6(b)]. Energy cost from B_s-Si_i^{T+} to B_{inty}^{B+} is found to be 0.81 (1.23) eV [Fig. 5(d)]. Further, for long distance diffusion, it is necessary for a Si interstitial to move to another nearby tetrahedral interstitial site with the boron being at the substitutional site. The calculated energy barrier for this rotation of the self-interstitial is about 1.1 eV, a little higher than the pair diffusion pathway involving B_i^{H+}. The diffusion of B with positively charged state is summarized in Fig. 7(a).

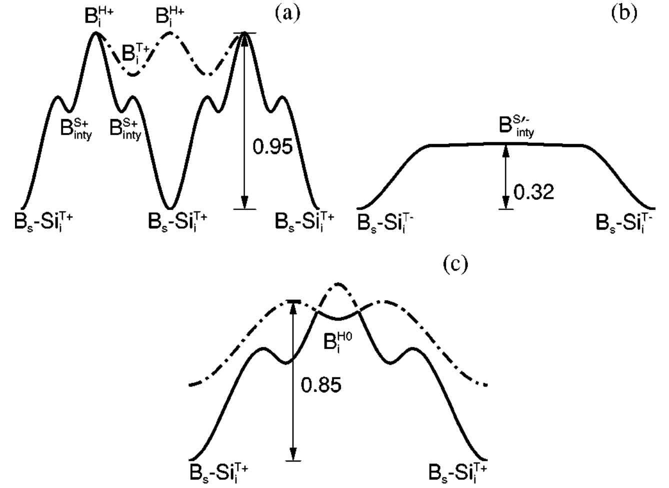

FIG. 7. Illustrations of relevant diffusion pathways and activation energies. The vertical axis is energy in eV and the horizontal axis is the configuration coordinates. (a) The diffusion for the positively charged state. There are two plausible pathways: the kick-out pathway (a dot-dashed line) and the pair diffusion pathway (a solid line). (b) The diffusion for the negatively charged state. (c) Recombination enhanced diffusion with the capture of a single electron. The dot-dashed line is for the diffusion without the electron capture and the solid line is for the recombination enhanced diffusion. In (c), the energy profiles are obtained with the Fermi level $\varepsilon_F = \varepsilon_v + 0.6$ eV.

It is of interest that the GGA and the LDA results for the total energy profiles are substantially different to each other although qualitative features are common. The obtained total energy profile for the process B_s-$Si_i^{T+} \rightarrow B_i^{H+} \rightarrow B_s$-$Si_i^{T+}$ is similar to the results from the previous GGA calculations.[21]

We next examine the diffusion of B with the neutral charge state. Again the diffusion starts from the most stable configuration B_s-Si_i^{T0}. Figures 5(e) and 5(f) show calculated total energy profiles from B_s-Si_i^{T0} to B_i^{H0} and to B_i^{T0}, respectively. We have found that the pathway along B_s-Si_i^{T0} to B_i^{H0} has definitely lower activation energy compared with that along B_s-Si_i^{T0} to B_i^{T0}: The calculated activation energy for B_s-Si_i^{T0} to B_i^{H0} is 0.40 (0.70) eV, whereas the value for B_s-Si_i^{T0} to B_i^{T0} is 0.83 (1.01) eV. Further, it is found that the activation energy along the interstitial channel is 0.28 (0.38) eV, whereas the energy barrier for the kick-in process from B_i^{H0} to B_s-Si_i^{T0} is 0.11 (0.19) eV. As for the diffusion via the bond-center configuration, it is found that the formation energy of B_{inty}^{B0} is relatively high, 0.67 eV in the GGA, indicating the bond-center diffusion process is irrelevant for the neutral charge state. It is thus reasonable to conclude that B with neutral charge state migrates via the pair diffusion mechanism, B_s-$Si_i^{T0} \rightarrow B_i^{H0} \rightarrow B_s$-$Si_i^{T0}$ and so forth.

The conclusion that the pair diffusion is important for the positive and neutral charge states has been already claimed by the previous calculations.[20,21] However, the conclusion is

only corroborated by the present comparison among the pair diffusion process, the bond-center diffusion process, and the kick-out and kick-in processes for different charge states.

As for the negatively charged states, the most stable configuration is B_{inty}^{A-}. The starting point for the diffusion is thus this configuration: The B_i^{X-} configuration identified as the most stable configuration in the past[21] is found to be only metastable. As a result, the diffusion pathway and corresponding activation energies obtained in the present work is quite different from the results in the past. First, the configuration B_{inty}^{S-} previously identified as the saddle point configuration[21] along the diffusion pathway has comparatively high activation energy 0.62 (0.71) eV [Fig. 5(h)]. Successive migration $B_{inty}^{S-} \rightarrow B_i^{H-} \rightarrow B_{inty}^{S-}$ has a barrier of 0.38 (0.45) eV [Fig. 5(i)]. We have found another appropriate saddle point configuration $B_{inty}^{S'}$ [Fig. 6(c)]. It has been clarified that the most plausible pathway for the negatively charged state is $B_{inty}^{A} \rightarrow B_{inty}^{S'} \rightarrow B_{inty}^{A} \rightarrow \cdots$ with the activation energy of 0.32 (0.41) eV [Fig. 5(g)]. This situation is illustrated in Fig. 7(b).

Now we have found that the diffusion pathways and corresponding activation energies are rather sensitive to the charge state of the diffusing species. This opens a possibility of charge-state dependent or recombination enhanced or retarded B diffusion. For instance, when the positively charged B_s-Si_i^{T+} captures an electron during the migration, it becomes the neutral B interstitial, B_i^H or B_i^T. When we consider this recombination process, the activation energy decreases from 0.95 eV to 0.85 eV [Fig. 7(c)] when the Fermi level is located at $\varepsilon_v + 0.6$ eV.

Finally, we briefly discuss on migration length λ. Experimentally, the temperature dependence of λ follows an Ahrenius plot with the activation energy of E_λ: $\lambda \propto \exp[-E_\lambda/(k_B T)]$. Cowern *et al.*[11] measured the value as $E_\lambda = -0.4$ eV. When we consider the pair diffusion process, E_λ is given by $2E_\lambda = E_m - E_{diss}$, where E_m and E_{diss} are the migration and dissociation energies of the pair. We evaluate these values and obtain $E_\lambda = -0.61(-0.65)$ eV when ε_F is in the middle of the gap. On the other hand, when we consider the kick-out mechanism, E_λ is given by $2E_\lambda = E'_m - E_{kin}$, where E'_m and E_{kin} are the migration energy of the interstitial B and the kick-in barrier to the substitutional site. We obtain $E_\lambda = 0.04$ eV in the GGA in this case. Therefore the pair diffusion mechanism seems to be more probable than the kick-out mechanism, though their activation energies are found to be comparable for the positively charged state.

IV. CONCLUSIONS

We have performed extensive first-principles total energy calculations for boron-silicon interstitial complexes with various configurations and charge states using the density functional theory. We have found that there are several stable and metastable configurations depending on the charge state. The most stable configuration is a pair of a substitutional B and an interstitial Si (B_s-Si_i^T) for positively charged state, whereas an interstitialcy configuration B_{inty}^{A} is the most stable for negatively charged state. The formation energy of the neutral B_{inty}^{A} is higher than that of B_s-Si_i^T only by 70 meV in the GGA, inferring that the substantial portion of neutral B takes the form of B_{inty}^{A}. From analyses of Kohn-Sham orbitals, it is proposed that the neutral B_{inty}^{A} is the microscopic origin of the EPR center experimentally observed in the past. Our GGA calculations also show that the B-Si complex is a negative-U system in which neutral charge states are only metastable with the Fermi energy at any position in the energy gap. Further, we have clarified diffusion pathways and corresponding activation energies for the B-Si complex. It is found that the boron is likely to diffuse in Si crystal as a form of a B-Si pair. However, the diffusion pathways and the activation energies are sensitive to the charge state, opening a possibility of recombination enhanced diffusion.

ACKNOWLEDGMENTS

We deeply thank Professor G. D. Watkins for valuable comments. Computations were performed by VPP500 and SR8000 at Institute for Solid State Physics (University of Tokyo), by SX4 and VPP5000 at Institute for Molecular Science (Okazaki), and by SX4 at Tohoku University. This work was supported in part by JSPS under Contract No. RFTF96P00203. The Grant-in-Aid for Scientific Research from the Ministry of Education, Science, and Culture in Japan under Contract No. 09NP1201 is also appreciated.

*Present Address: Electronics and Telecommunication Research Institute, Taejon 305-350, Korea.

[1] W. Frank, U. Gösele, H. Mehrer, and A. Seeger, in *Diffusion in Crystalline Solids*, edited by G. E. Murch and A. S. Nowick (Academic Press, New York, 1984), p. 63.

[2] P.M. Fahey, P.B. Griffin, and J.D. Plummer, Rev. Mod. Phys. **61**, 289 (1989).

[3] *Defects and Diffusion in Silicon Processing*, edited by T. Diaz de la Rubia *et al.*, MRS Symposia Proceedings No. 469 (Materials Research Society, Pittsburgh, 1997).

[4] K.C. Pandey, Phys. Rev. Lett. **57**, 2287 (1986).

[5] K.C. Pandey and E. Kaxiras, Phys. Rev. Lett. **66**, 915 (1991).

[6] R. Car, P.J. Kelly, A. Oshiyama, and S.T. Pantelides, Phys. Rev. Lett. **52**, 1814 (1984).

[7] C.S. Nichols, C.G. Van de Walle, and S.T. Pantelides, Phys. Rev. Lett. **62**, 1049 (1989); Phys. Rev. B **40**, 5484 (1989).

[8] R. Car, P.J. Kelly, A. Oshiyama, and S.T. Pantelides, Phys. Rev. Lett. **54**, 360 (1985).

[9] O. Sugino and A. Oshiyama, Phys. Rev. B **46**, 12 335 (1992).

[10] P.E. Blöchl, E. Smargiassi, R. Car, D.B. Laks, W. Andreoni, and S.T. Pantelides, Phys. Rev. Lett. **70**, 2435 (1993).

[11] E.B. Cowern, K.T.F. Janssen, G.F.A. van de Walle, and D.J. Gravesteijn, Phys. Rev. Lett. **65**, 2434 (1990).

[12] N.E.B. Cowern, G.F.A. van de Walle, D.J. Gravesteijn, and C.J.

Vriezema, Phys. Rev. Lett. **67**, 212 (1991).
[13] H. Bracht, E.E. Haller, and R. Clark-Phelps, Phys. Rev. Lett. **81**, 393 (1998).
[14] A. Ural, P.B. Griffin, and J.D. Plummer, Phys. Rev. Lett. **83**, 3454 (1999).
[15] U. Gösele and T. Y. Tan, in *Defects in Semiconductors II*, edited by J. W. Corbett and S. Mahayan (North-Holland, New York, 1983), p. 45.
[16] A. Ural, P.B. Griffin, and J.D. Plummer, J. Appl. Phys. **85**, 6440 (1999).
[17] J. Zhu, T. Diaz de la Rubia, L.H. Yang, C. Manilhiot, and G.H. Gilmer, Phys. Rev. B **54**, 4741 (1996).
[18] J. Zhu, in *Defects and Diffusion in Silicon Processing*, edited by T. Diaz de la Rubia *et al.*, MRS Symp. Proc. No. 469 (Materials Research Society, Pittsburgh, 1997), p. 151.
[19] J. Zhu, Comput. Mater. Sci. **12**, 309 (1998).
[20] B. Sadigh, T.J. Lenosky, S.K. Theiss, M.-J. Caturla, T. Diaz de la Rubia, and M.A. Foad, Phys. Rev. Lett. **83**, 4341 (1999).
[21] W. Windl, M.M. Bunea, R. Stumpf, S.T. Dunham, and M.P. Masquelier, Phys. Rev. Lett. **83**, 4345 (1999).
[22] G. Kresse and J. Furthmüller, *VASP the Guide* (Vienna University of Technology, Vienna, 1999).
[23] A simplified version of the LDA (the regional energy convergence approximation) is used to obtain stable structures of B in Si: E. Tarnow, Europhys. Lett. **16**, 449 (1991).
[24] M. Hakala, M.J. Puska, and R.M. Nieminen, Phys. Rev. B **61**, 8155 (2000).
[25] P.W. Anderson, Phys. Rev. Lett. **34**, 953 (1975).
[26] G.A. Baraff, B.O. Kane, and M. Schlüter, Phys. Rev. Lett. **43**, 956 (1979).
[27] G.D. Watkins and J.R. Troxell, Phys. Rev. Lett. **44**, 593 (1980); J.R. Troxell and G.D. Watkins, Phys. Rev. B **22**, 921 (1980).
[28] R.D. Harris, J.L. Newton, and G.D. Watkins, Phys. Rev. Lett. **48**, 1271 (1982); R.D. Harris, J.L. Newton, and G.D. Watkins, Phys. Rev. B **36**, 1094 (1987).
[29] G.D. Watkins, Phys. Rev. B **12**, 5824 (1975).
[30] P. Hohenberg and W. Kohn, Phys. Rev. **136**, B864 (1964); W. Kohn and L.J. Sham, Phys. Rev. **140**, A1133 (1965).
[31] G.B. Bachelet, D.R. Hamann, and M. Schlüter, Phys. Rev. B **26**, 4199 (1982).
[32] N. Troullier and J.L. Martins, Phys. Rev. B **43**, 1993 (1991).
[33] L. Kleinman and D.M. Bylander, Phys. Rev. Lett. **48**, 1425 (1982).
[34] J.P. Perdew, J.A. Chevary, S.H. Vosko, K.A. Jackson, M.R. Perderson, D.J. Singh, and C. Fiolhais, Phys. Rev. B **46**, 6671 (1992); **48**, 4978 (1993).
[35] J.P. Perdew and A. Zunger, Phys. Rev. B **23**, 5048 (1981).
[36] D.M. Ceperley and B.J. Alder, Phys. Rev. Lett. **45**, 566 (1980).
[37] The cutoff energy of the plane-wave basis set has been determined by performing total energy calculations for a B interstitial atom in Si with cutoff energies up to 56 Ryd. The total energy obtained with the 28-Ryd cutoff differs from the converged value by 3 meV per atom.
[38] O. Sugino and A. Oshiyama, Phys. Rev. Lett. **68**, 1858 (1992).
[39] M.P. Teter, M.C. Payne, and D.C. Allan, Phys. Rev. B **40**, 12 255 (1989).
[40] D.M. Bylander, L. Kleinman, and S. Lee, Phys. Rev. B **42**, 1394 (1990).
[41] C.-O. Almbladh and U. von Barth, Phys. Rev. B **31**, 3231 (1985).
[42] J. C. Slater, *The Self Consistent Field for Molecules and Solids* (McGraw-Hill, New York, 1974).
[43] G.A. Baraff, E.O. Kane, and M. Schluter, Phys. Rev. B **21**, 5662 (1980).
[44] S. Jeong and A. Oshiyama, Phys. Rev. Lett. **81**, 5366 (1998).
[45] It is not clear that the present method of searching diffusion pathways is superior to the nudged elastic band method which is used in Reference 21. The two ways seem to be similar to each other in principle.